

Evaluation of Wall Boundary Condition Parameters for Gas–Solids Fluidized Bed Simulations

Tingwen Li

National Energy Technology Laboratory, U.S. Department of Energy, Morgantown, WV 26507

URS Corporation, Morgantown, WV 26505

Sofiane Benyahia

National Energy Technology Laboratory, U.S. Department of Energy, Morgantown, WV 26507

DOI 10.1002/aic.14132

Published online May 16, 2013 in Wiley Online Library (wileyonlinelibrary.com)

*Wall boundary conditions for the solids phase have significant effects on numerical predictions of various gas–solids fluidized beds. Several models for the granular flow wall boundary condition are available in the open literature for numerical modeling of gas–solids flow. A model for specular coefficient used in Johnson and Jackson boundary conditions by Li and Benyahia (Li and Benyahia, *AIChE J.* 2012;58:2058–2068) is implemented in the open-source CFD code-MFIX. The variable specular coefficient model provides a physical way to calculate the specular coefficient needed by the partial-slip boundary conditions for the solids phase. Through a series of two-dimensional numerical simulations of bubbling fluidized bed and circulating fluidized bed riser, the model predicts qualitatively consistent trends to the previous studies. Furthermore, a quantitative comparison is conducted between numerical results of variable and constant specular coefficients to investigate the effect of spatial and temporal variations in specular coefficient. Published 2013 American Institute of Chemical Engineers *AIChE J.* 59: 3624–3632, 2013*

Keywords: computational fluid dynamics, fluidized bed, gas–solids flow, boundary condition, granular flow, two-fluid model

Introduction

With the recent, fast development in computational power and numerical algorithms, computational fluid dynamics (CFD) has become a very effective complementary tool for experiments to understand the complex hydrodynamics of gas–solids flows encountered in many industrial applications, including energy production and chemical, pharmaceutical, food, and agricultural processing. CFD is playing an important role in optimizing the design and operation of these industrial processes.

A number of CFD modeling approaches exist for gas–solids flows covering different scales.¹ Among them, the Lagrangian–Eulerian (LE) method, and the Eulerian–Eulerian (EE) method or two-fluid model (TFM) are the most widely used approaches for simulating gas–solids flows. For simulations using either the LE or EE method, appropriate wall boundary conditions are crucial to the quantitative prediction of gas–solid flows. For the gas phase, a no-slip wall boundary condition is usually applied in gas–solids flow simulations, and this is believed to be reasonable for most cases. However, the boundary condition for the solids phase is not as straightforward in the EE method as it is in the LE

method. In the EE modeling, different wall boundary conditions for the solids phase can be found in the literature, including free-slip, partial-slip, and no-slip boundary conditions. Among the aforementioned boundary conditions for the solids phase, partial-slip boundary conditions are considered to be the most realistic. Various models for the granular flow partial-slip wall boundary condition are available in the open literature.^{2–4} The boundary conditions proposed by Johnson and Jackson² have been widely applied in numerical simulations of gas–solids flows in various fluidized beds due to their physical base and relatively simple form.

In Johnson and Jackson boundary conditions, the specular coefficient that characterizes the collisional tangential momentum transfer between the solids flow and the wall is an important input parameter for numerical simulations. The specular coefficient ranges from 0 to 1, with a zero value for perfectly specular collisions (particles slipping freely at walls) and a value of unity for perfectly diffuse collisions (particles sticking or not slipping at walls). Different specular coefficients have been adopted in the literature with high values (~0.5) most common in simulating bubbling fluidized beds, while low values are applied to circulating fluidized bed simulations. Several studies have demonstrated that the flow field is very sensitive to the specular coefficient.^{5–10} Benyahia et al.⁵ evaluated the effect of boundary conditions used to model the dilute turbulent gas–solids pipe flow and found that a small specular coefficient is preferential for the simulated problem. Almuttahir and Taghipour¹¹ investigated the effect

Correspondence concerning this article should be addressed to T. Li at tingwen.li@contr.netl.doe.gov

Published 2013 American Institute of Chemical Engineers
This is a U.S. Government work and, as such, is in the public domain in the United States of America.

of several model parameters in two-dimensional (2-D) numerical simulations of a high-density circulating fluidized bed riser. They reported that the specular coefficient influenced the solids concentration distribution, and a zero value for this parameter led to good agreement with the experimental data. Wang et al.¹⁰ and Jin et al.⁶ carried out EE numerical simulations of the hydrodynamic behaviors of high-flux circulating fluidized beds with Geldart group A and group B particles and conducted a comprehensive sensitivity study of key model parameters. They found that the specular coefficient has a slight effect on the gas velocity and solids velocity distributions but a pronounced effect on the solids volume fraction distribution for both types of particles. A numerical study of gas mixing in gas–solids fluidized bed by Li et al.⁹ revealed that the solids-phase wall boundary condition needs to be specified with great care when predicting the gas mixing. Substantial differences were observed in the gas backmixing when varying the specular coefficient. When the specular coefficient is carefully chosen to fit the axial and radial tracer concentration measured in the experiment, a lower value of specular coefficient tends to be appropriate for the same system operated under higher superficial gas velocity. A similar phenomenon was observed by Li et al.⁸ in simulating a pseudo-2-D bubbling fluidized bed where the specular coefficient was found to affect the solids flow behavior significantly and likely to be dependent on the flow conditions. Lan et al.⁷ studied the influence of solids-phase wall boundary condition in terms of specular coefficient and particle–wall restitution coefficient on the flow behavior of spouted beds in EE simulations. The simulated results show that the solids-phase wall boundary condition plays an important role in CFD modeling of spouted beds. The specular coefficient has a pronounced effect on the spouting behavior, and a small specular coefficient (0.05) yields reasonable predictions.

Clearly, choosing the correct value of specular coefficient is critical for most validation studies because the wall effect is believed to be more important for small-scale laboratory systems than large-scale industrial plants. To determine this parameter, Hui et al.¹² recommended that tangential velocity changes should be measured for a large number of collisions with different impact velocities and impact angles on a representative section of the wall. However, no such measurement has been reported in the literature. One way to specify the specular coefficient is to adjust this parameter to fit some experimental data. However, this is unlikely to be feasible for large-scale fluidized bed simulations where the experimental measurements are very limited and the computation is highly time-consuming. In addition, as suggested by the previous studies^{8,9}, the specular coefficient fitted with certain experimental data may not work universally for the same system under different flow conditions. To overcome these issues, Li and Benyahia¹³ revisited the Johnson and Jackson boundary conditions and derived a working expression for the specular coefficient based on the properties of particle–wall collision and flow behavior. This model provides a physical way to calculate the specular coefficient as a field variable along the wall; hence, it is of practical interest to investigate the validity and performance of this model in numerical simulations of gas–solids fluidization systems.

The objective of this study is to evaluate the recent model of specular coefficient for Johnson and Jackson boundary conditions proposed by Li and Benyahia¹³ implemented in

the open-source code MFIX. Performance of this variable specularity model is evaluated through a series of 2-D numerical simulations of a bubbling fluidized bed and a circulating fluidized bed riser. The interactions between flow conditions and the specular coefficient are investigated qualitatively. In addition, the numerical results of constant and variable specular coefficients are compared in terms of accuracy and computational speed.

Numerical Model

The multiphase continuum flow solver of an open-source code, MFIX, is used. Mass and momentum conservation equations are solved for the gas and solids (particulate) phases with the appropriate closure relations. Specifically, the governing equations for the solids phase are closed by granular kinetic theory. A partial differential equation for granular temperature is solved to model the fluctuating energy of the solids phase. The drag correlation proposed by Gidaspow, which is a combination of Wen and Yu and Ergun correlations, is used to describe the interphase interaction between gas and solids. Governing equations solved in MFIX are summarized by Benyahia et al.¹⁴. More details on theory and numerical techniques in MFIX can be found at <https://mfix.netl.doe.gov>^{15,16}.

The following boundary conditions for the solids phase developed by Johnson and Jackson² has been implemented in MFIX

$$\frac{\vec{V}_{sl} \cdot (\bar{\sigma}_p) \cdot \vec{n}}{|\vec{V}_{sl}|} + \frac{\phi \sqrt{3\Theta} \pi \rho_p \alpha_p |\vec{V}_{sl}| g_0}{6\alpha_{p,max}} + N_f \tan \delta = 0 \quad (1)$$

The first term on the left side of Eq. 1 denotes the stress in the solids flow on approaching the wall. Here, \vec{V}_{sl} is the slip velocity between the particles and the wall, $\bar{\sigma}_p$ is the solids stress tensor, and \vec{n} is the unit normal vector to the wall. The second term stands for the rate of tangential momentum transfer to the wall by particle–wall collisions. ϕ is the specularity coefficient, ρ_p is the density of the solids material, Θ is the granular temperature, g_0 is the radial distribution function, α_p is the solids volume fraction, and $\alpha_{p,max}$ is the solids volume fraction at a closely random packing state. The third term on the left side of Eq. 1 is the stress due to sliding particles, which is obtained by applying Coulomb's law of friction to the particles sliding over the surface. N_f is the normal frictional component of stress (i.e., the frictional pressure), and δ is the angle of friction between the wall surface and the particles.

For the fluctuation energy (or granular energy), Johnson and Jackson² derived the following boundary condition

$$-\vec{n} \cdot \vec{q}_{PT} = D + \vec{V}_{sl} \cdot \vec{S}_c^b \quad (2)$$

where \vec{q}_{PT} is the flux of fluctuation energy and D is the rate of dissipation of fluctuation energy due to inelastic particle–wall collisions expressed as

$$D = \frac{1}{4} \pi \rho_p \alpha_p \Theta (1 - e_w^2) g_0 \frac{\sqrt{3\Theta}}{\alpha_{p,max}} \quad (3)$$

where e_w is the normal restitution coefficient of particle–wall collisions. \vec{S}_c^b is the force per unit area on the wall due to particle–wall collisions given by

$$S_c^b = \frac{\phi \sqrt{3\Theta} \pi \rho_p \alpha_p \vec{V}_{sl} g_0}{6\alpha_{p,max}} \quad (4)$$

In Johnson and Jackson boundary conditions, the specular coefficient, ϕ , must be specified to characterize the tangential momentum transfer due to collisions.

Li and Benyahia¹³ revisited Johnson and Jackson boundary conditions for granular flows by adopting the classic rigid-body theory for the particle–wall collision and kinetic theory to determine the dependence of the specular coefficient on particle–wall collision properties and flow behavior. By assuming thermodynamic equilibrium close to the wall, a working expression for the specular coefficient, derived by Li and Benyahia from numerical integration based on the isotropic Maxwellian velocity distribution, is provided below for a general problem and only requires knowledge of normal particle–wall restitution coefficient and wall friction coefficient. Ignoring the angular velocity of particles, which is not available in most EE modeling, the specular coefficient can be calculated by the following equation

$$\phi = \begin{cases} -\frac{7\sqrt{6\pi}(\phi_0)^2}{8k}r + \phi_0 & r \leq \frac{4k}{7\sqrt{6\pi}\phi_0} \\ \frac{2}{7} \frac{k}{r\sqrt{6\pi}} & \text{otherwise} \end{cases} \quad (5)$$

where $r = u/\sqrt{3\Theta}$ is the normalized slip velocity at the wall characterizing the mean impact angle of particles with $u = |\vec{V}_{sl}|$, and $k = \frac{7}{2}\mu_f(1+e_w)$ is a combination of friction coefficient, μ_f , and the normal particle–wall restitution coefficient, e_w . ϕ_0 is the value of ϕ when r tends to zero. For the range of $k \in (0, 10)$ of practical interest, an approximate equation of ϕ_0 is suggested.

$$\begin{aligned} \phi_0 = & -0.0012596 + 0.1064551k - 0.04281476k^2 \\ & + 0.0097594k^3 - 0.0012508258k^4 \\ & + 0.0000836983k^5 - 0.00000226955k^6 \end{aligned} \quad (6)$$

In a previous study by Li and Benyahia, this model was verified against the previous study by Jenkins³, as well as the numerical results from particle simulations by Louge¹⁷. This model for specular coefficient has been implemented recently and is available in the MFIx open-source code. In this numerical code, the specular coefficient at each wall cell is first calculated based on the flow conditions and physical properties and then used in the Johnson and Jackson partial-slip boundary conditions during gas–solids flow simulations.

Simulation Setup

To save computational time, only 2-D numerical simulations are conducted. Two cases including a bubbling fluidized bed and a circulating fluidized bed riser as schematically shown in Figure 1 are considered in the current study. As this study only considers 2-D simulations, and physical experiments are naturally three-dimensional (3-D), no attempts to compare against experimental data will be conducted. It should be emphasized that the objective of this study is to evaluate the performance of this variable specular coefficient model and to investigate how the specular coefficient affects the numerical results.

The first case is a 2-D bubbling fluidized bed with 0.75 m height and 0.25 m width. Glass beads with particle diameter

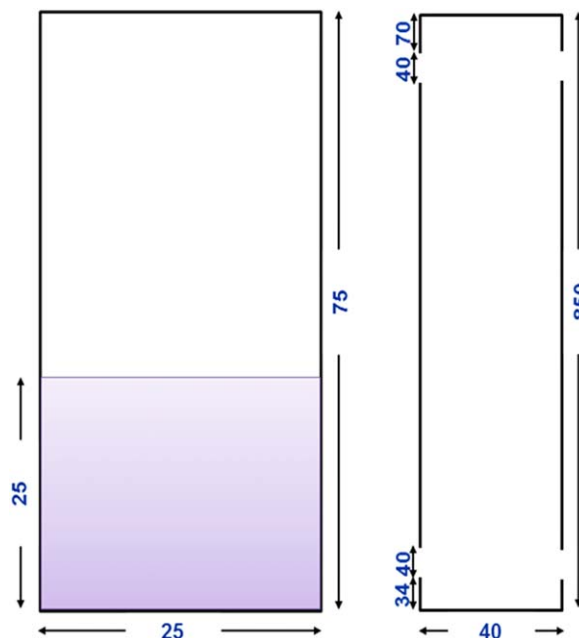


Figure 1. Schematic of (a) bubbling fluidized bed and (b) circulating fluidized bed riser (unit: cm).

[Color figure can be viewed in the online issue, which is available at wileyonlinelibrary.com]

of 400 μm and density of 2500 kg/m^3 are fluidized with different superficial gas velocities of 0.2, 0.3, and 0.6 m/s, respectively. Two particle–wall friction coefficients are tested to study the flow behavior under different wall properties. Both constant and variable specular coefficients are tested in the Johnson and Jackson partial-slip boundary conditions. The specular coefficient is calculated based on Li and Benyahia¹³ at each wall cell and stored for post-analysis to evaluate the variation of specular coefficient with operating conditions and particle–wall properties. Uniform grid of 5 mm, which corresponds to 12.5 times the particle diameter, is used in all simulations and is believed to be grid-insensitive according to our previous grid-convergence study of similar configurations.⁸ The grid independence is further confirmed by a brief grid study using three grid sizes of 6.25 mm, 5 mm, and 4 mm. Detailed parameters used in the numerical simulation of bubbling fluidized beds are given in Table 1. Total simulation time of 60 s is completed for each case and mean flow field information are extracted from the last 50 s numerical results for analysis.

The second case is a circulating fluidized bed riser reported by Lu et al.¹⁸. The riser section is an 8.5 m tall cylindrical column with diameter of 0.4 m as shown in Figure 1b. For this case, 2-D numerical domain with two solids-inlets and outlets are used to achieve symmetric flow behavior¹⁹. Particles with diameter of 300 μm and density of 2500 kg/m^3 are circulated by a superficial gas velocity of 7.76 m/s under ambient conditions. Two solids circulation rates are studied with solids mass flux of 50 $\text{kg/m}^2\text{s}$ and 400 $\text{kg/m}^2\text{s}$, respectively. Table 2 summarizes detailed numerical parameters used in the simulations. A grid of 80×850 is used and is believed to be grid-insensitive according to a previous study of the same case.¹⁸ Numerical results of 80 s are analyzed with the first 25 s of numerical simulation excluded to avoid the startup effect.

Table 1. Parameters Used in the Numerical Simulations of Bubbling Fluidized Bed

Parameter	Value
Height	0.75 m
Grid size	0.005 m
Initial bed voidage	0.45
Particle density	2500 kg/m ³
Particle–particle restitution coefficient	0.95
Particle–wall friction coefficient	0.36, 0.09
Gas velocity	0.2, 0.3, 0.6 m/s
Viscosity	1.8×10^{-5} Pa s
Width	0.25 m
Initial bed height	0.25 m
Solid packing limit	0.6
Particle diameter	400 μ m
Particle–wall restitution coefficient	0.8
Total simulation time	60 s
Temperature	297 K
Pressure	1 atm

Numerical Results and Discussion

Bubbling fluidized bed

According to Li and Benyahia's model, the specularity coefficient is calculated for each wall cell at every time step. Figure 2a presents the spatial variation of specularity coefficient along the left wall at a specific time of the simulation. Along the wall, high values of specularity coefficient tend to be observed in regions near the bottom distributor and upper bed surface where the solids volume fraction is low and the granular temperature is high. Above the bed surface, no specularity coefficient is reported as no particle exists at that height. Figure 2b shows the time variation of specularity coefficient at one point on the left wall located at 0.15 m above the bottom distributor. The specularity coefficient fluctuates because of the local flow dynamics. At each time, the spatially averaged specularity coefficient along the left wall was calculated by averaging over all the wall cells. Figure 2c plots the time variation of this average specularity coefficient. An overall effective specularity coefficient of 0.0746 can be obtained by averaging this quantity over a time-period of 50 s. This overall effective specularity coefficient is consistent with the procedure proposed by Hui et al.¹² for measuring the specularity coefficient experimentally. Hence, it can be used as an input for the original Johnson and Jackson's boundary conditions for the solids phase.

An overall constant effective specularity coefficient of 0.0746 is used in the numerical simulation with the original Johnson and Jackson's wall boundary conditions for comparison. Figure 3 compares the distribution of mean voidage

Table 2. Parameters Used in the Numerical Simulations of Circulating Fluidized Bed Riser

Parameter	Value
Height	8.5 m
Particle density	2,500 kg/m ³
Particle–particle restitution coefficient	0.98
Particle–wall friction coefficient	0.577, 0.176
Gas velocity	7.76 m/s
Viscosity	1.8×10^{-5} Pa s
Width	0.4 m
Particle diameter	300 μ m
Particle–wall restitution coefficient	0.8
Total simulation time	80 s
Temperature	297 K
Pressure	1 atm

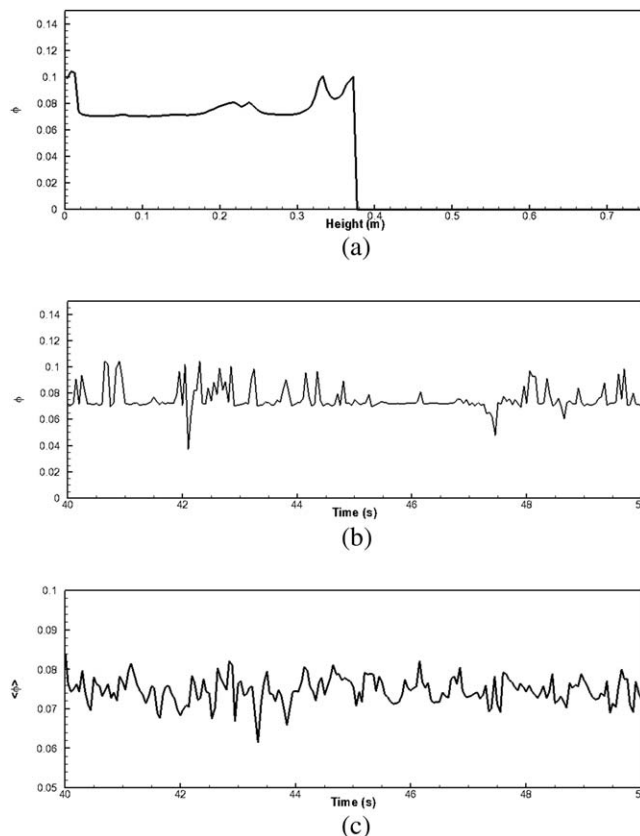


Figure 2. Spatial and temporal distribution of specularity coefficient (a) variation along the left wall at $t = 40$ s; (b) time variation at a point 0.15 m above the bottom distributor on the left wall; (c) time variation of the spatially averaged specularity coefficient ($U_g = 0.6$ m/s; $\mu_f = 0.36$).

and vertical solid velocity inside the computational domain. The results of a constant and variable specularity coefficient are very similar with only minor differences. Further comparison is made for the lateral profiles of mean voidage and solid vertical velocity at the height of 0.25 m above the distributor, as shown in Figure 4. The negligible differences between these two approaches of modeling suggest that a constant value for specularity coefficient can reasonably capture the particle–wall interaction in a bubbling fluidized bed. This conclusion can be justified by the small temporal and spatial variation in the specularity coefficient as shown in Figure 2.

Only two material properties affect the specularity coefficient: the normal particle–wall restitution coefficient and particle–wall friction coefficient, with the latter having a stronger effect than the former, according to Li and Benyahia's analysis. The friction coefficient is determined by both particle and wall physical properties, as well as wall roughness. Here, two friction coefficients of 0.36 and 0.09 are tested, which leads to different specularity coefficients and different flow hydrodynamics. Figure 5 presents the mean flow fields of voidage and solids vertical velocity for the superficial gas velocity of 0.6 m/s. Clearly, the flow hydrodynamics are quantitatively different. From the solids velocity distribution, a stronger solids backmixing along the wall is observed for lower particle–wall friction. For a low friction

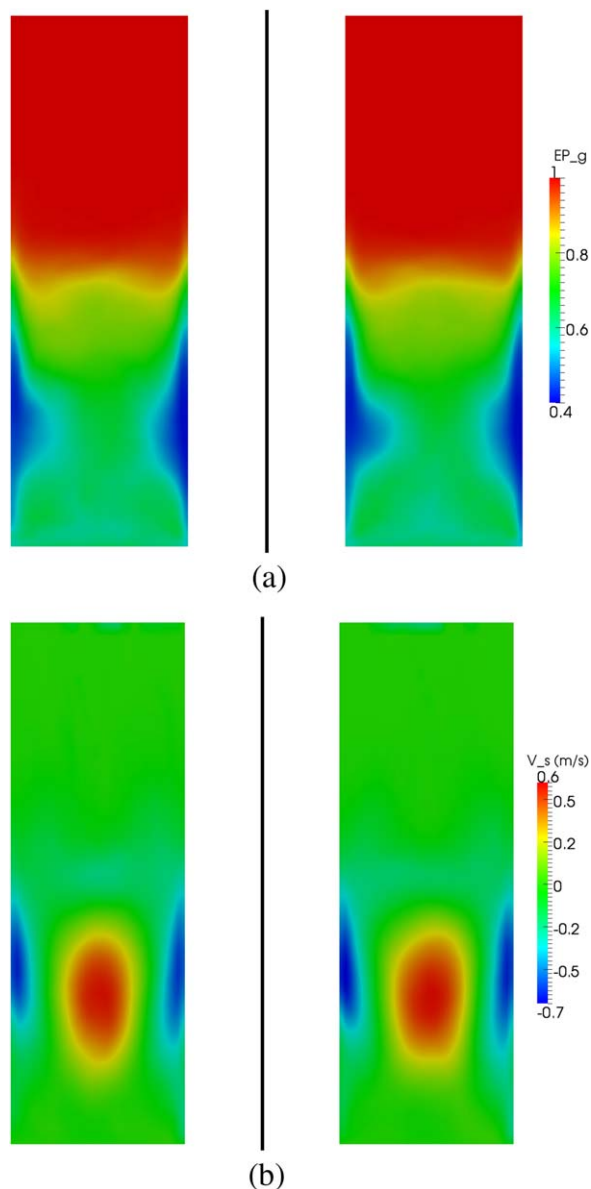


Figure 3. Comparison of distributions of (a) mean voidage and (b) vertical solids velocity (Left: variable specularity coefficient.

Right: constant specularity coefficient) ($U_g = 0.6$ m/s; $\mu_f = 0.36$). [Color figure can be viewed in the online issue, which is available at wileyonlinelibrary.com]

coefficient of 0.09, the overall effective specularity coefficient is 0.0088, which is about an order of magnitude smaller than that of 0.0746, for the case with a high friction coefficient of 0.36.

As discussed in previous studies, fluidized bed operating conditions seem to affect the specularity coefficient (e.g., the superficial gas velocity). In the current study, three superficial gas velocities are studied and the overall specularity coefficient is observed to decrease slightly as the superficial gas velocity increases (shown in Table 3), which is consistent with the finding reported in the literature.⁹ The overall specularity coefficients obtained here were used as input parameters for additional simulations, which produced results consistent with the variable specularity coefficient model.

Circulating fluidized bed riser

Parametric study for the specularity coefficient is carried out first for the circulating fluidized bed riser in which fixed specularity coefficients values of 0, 0.0005, 0.002, 0.01, 0.05, 0.2, 0.5, and 1 are used. Figure 6 shows the radial profiles of mean voidage and solids vertical velocity in the middle of riser predicted by all different specularity coefficients. A symmetric core-annular flow pattern is predicted for all cases; however, different specularity coefficients for the solids-phase wall boundary lead to quantitative differences. Overall, the inner flow field is relatively insensitive to the choice of specularity coefficient, and its influence is limited to the wall region especially for the solids velocity profiles. Hence, it is of interest to focus only on the flow field information in the wall region to evaluate the effect of the specularity coefficient. Figure 7 compares axial profiles of mean voidage and vertical solids velocity along the riser wall, predicted by different specularity coefficients. For the sake of clarity, only four cases with specularity coefficient of 0, 0.002, 0.2, and 1 are shown in the plots. It can be seen that both voidage and solids velocity are affected by the choice of this parameter. However, the solids velocity along the wall shows more sensitivity to the specularity coefficient, which will inevitably affect the solids backmixing and reactor performance. In most regions, the results by specularity coefficient of 0 and 1, corresponding to free-slip and no-slip

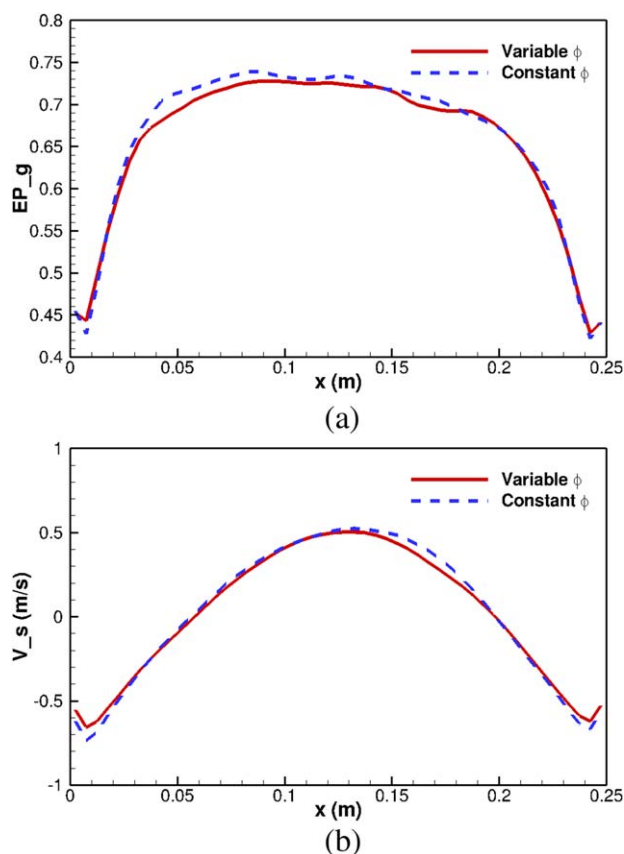


Figure 4. Comparison of the time-averaged lateral profiles of (a) voidage and (b) vertical solids velocity for variable and constant specularity coefficient ($U_g = 0.6$ m/s; $\mu_f = 0.36$).

[Color figure can be viewed in the online issue, which is available at wileyonlinelibrary.com]

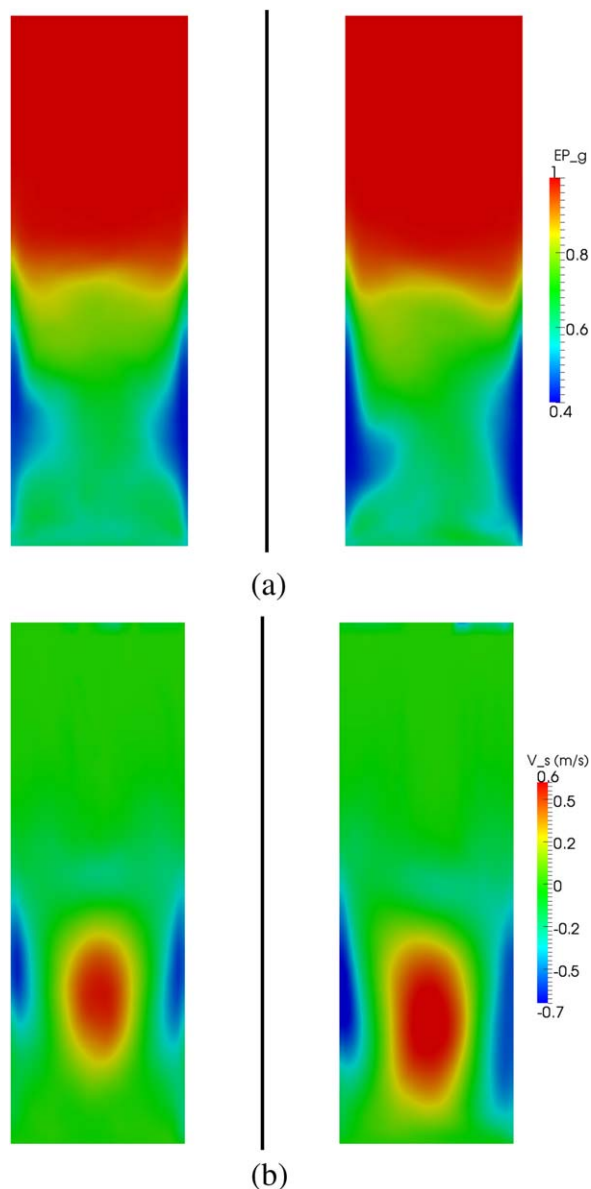


Figure 5. Comparison of time-averaged distributions of (a) voidage and (b) vertical solids velocity for different particle-wall friction coefficient (Left: high friction. Right: low friction. $U_g=0.6$ m/s).

[Color figure can be viewed in the online issue, which is available at wileyonlinelibrary.com]

boundary conditions, respectively, tend to bind the overall results. However, this does not hold true for all regions, such as the solids concentration in the lower region above the solids inlet. One possible reason is the simulation time is not long enough to time average the data even though this is

Table 3. Overall Specularity Coefficient and its Standard Deviation for Cases with Different Superficial Gas Velocities

Superficial gas velocity	$U_g = 0.2$ m/s	$U_g = 0.3$ m/s	$U_g = 0.6$ m/s
Overall mean specularity	0.0809	0.077	0.0746
Standard deviation	0.00368	0.00315	0.00345

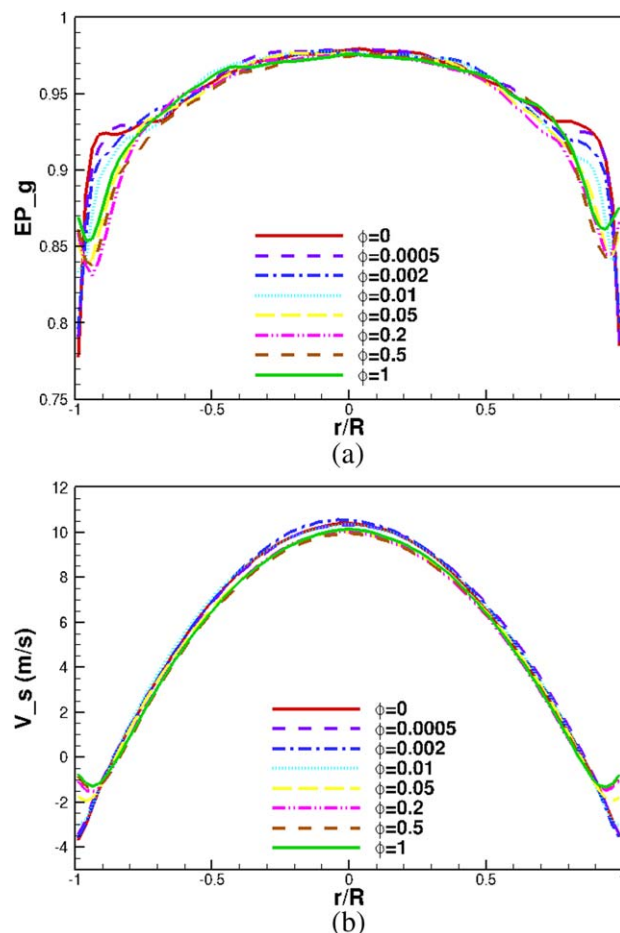


Figure 6. Time-averaged radial profiles of (a) voidage and (b) vertical solids velocity in the middle of riser predicted by different specularity coefficients.

[Color figure can be viewed in the online issue, which is available at wileyonlinelibrary.com]

usually the typical simulation duration in most numerical studies. On the other hand, it should be noted that the interaction of the solids flow and the wall is complex and may not exhibit monotonous behavior with respect to the specularity coefficient. Nevertheless, the results presented in this study show clear differences in near-wall behavior for different values of specularity coefficient.

Next, a similar study at higher solids mass flux has been carried out in the same circulating fluidized bed riser for which the variable specularity coefficient is used. Three particle-wall friction coefficients of 0.58, 0.364, and 0.176 are tested for the case with a solids flux of $400 \text{ kg/m}^2\text{s}$. The distributions of time-average specularity coefficient over the last 60 s of simulation along the wall for different friction coefficients are shown in Figure 8. Clearly, the specularity coefficient increases with the wall friction coefficient. In addition, low friction tends to show more variation in the mean specularity coefficient along the wall. Overall, the spatial variation of mean specularity coefficient along the wall is moderate.

Solids circulation rate is one of the major operating conditions of circulating fluidized bed affecting the flow hydrodynamics inside the riser, which may influence the mean specularity coefficient profiles along the wall. To evaluate

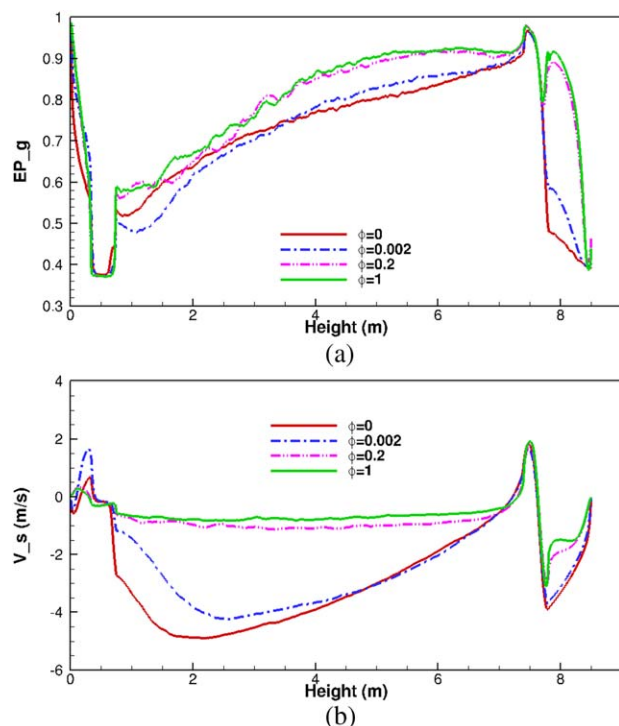


Figure 7. Time-averaged axial profiles of (a) voidage and (b) vertical solids velocity along the riser wall predicted by different specularity coefficients.

[Color figure can be viewed in the online issue, which is available at wileyonlinelibrary.com]

this influence, the mean specularity coefficient distribution along the wall of a low solids circulation rate with solids mass flux of $50 \text{ kg/m}^2\text{s}$ is compared to the results of high solids circulation rate for different friction coefficients (see Figure 9). This comparison shows that the solids circulation rate does affect the distribution of mean specularity coefficient. However, the specularity coefficient is more sensitive to the friction coefficient than the solids circulation rate. Again, for both solids circulation rates, the spatial variation of mean specularity coefficient is stronger for the low friction coefficient. The overall effective specularity coefficients are calculated for different cases and shown in Table 4; the

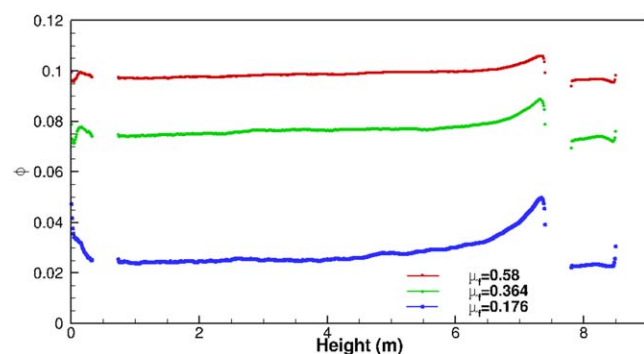


Figure 8. Variation of mean specularity coefficient along the wall for different friction coefficients ($U_g = 7.76 \text{ m/s}$, $G_s = 400 \text{ kg/m}^2\text{s}$).

[Color figure can be viewed in the online issue, which is available at wileyonlinelibrary.com]

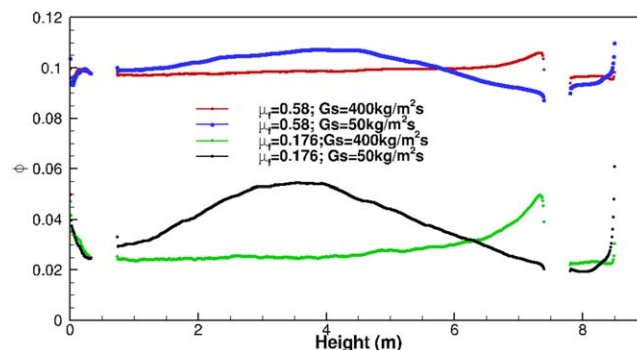


Figure 9. Variation of mean specularity coefficient along the wall for different friction coefficients and solids circulation rates.

[Color figure can be viewed in the online issue, which is available at wileyonlinelibrary.com]

Table 4. Overall Effective Specularity Coefficients for CFB riser Simulations with Different Solids Circulation Rates and Friction Coefficients

Solids flux/friction coefficient ($\text{kg/m}^2\text{s}$)	$\mu_r = 0.176$	$\mu_r = 0.58$
$G_s = 50$	0.0386	0.101
$G_s = 400$	0.0278	0.0988

overall effective specularity coefficient decreases slightly as the solids circulation rate is increased from $50 \text{ kg/m}^2\text{s}$ to $400 \text{ kg/m}^2\text{s}$.

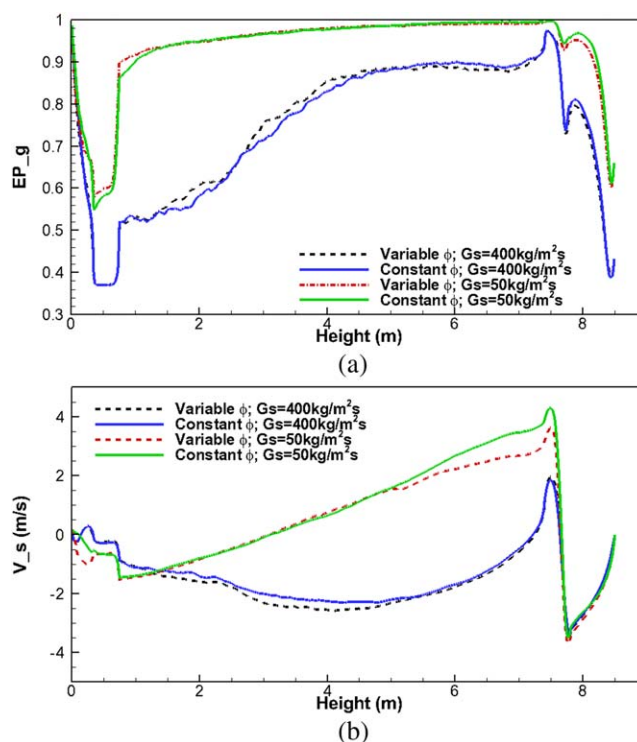


Figure 10. Time-averaged axial profiles of (a) voidage and (b) vertical solids velocity along the riser wall predicted with variable and constant specularity coefficients.

[Color figure can be viewed in the online issue, which is available at wileyonlinelibrary.com]

Table 5. Comparison of Computational Costs of Different Numerical Simulations

Simulation	Computing Time (s)		Additional Information
	Constant	Variable	
Bubbling bed ($U_g = 0.6\text{m/s}$)	187,640	174,402	60 s simulation on 1 Intel Xeon X5550 CPU core @ 2.67 GHz
CFB ($G_s = 50\text{ kg/m}^2\text{s}$)	206,515	194,508	80 s simulation on 16 Intel Xeon E5440 CPU cores @ 2.83GHz
CFB ($G_s = 400\text{ kg/m}^2\text{s}$)	385,513	380,827	80 s simulation on 16 Intel Xeon E5440 CPU cores @ 2.83GHz

Again, numerical results with constant specularity coefficients are compared against those with variable specularity coefficients. The overall effective specularity coefficient is calculated by spatial averaging the variable specularity coefficient over all wall cells and temporal averaging during the last 60 s of the simulation. The mean voidage and solids velocity along the wall are compared for simulations with variable and constant specularity coefficients for cases with different friction coefficients and solids circulation rates. Figure 10 shows the comparison for two solids circulation rates with low friction coefficient, which exhibited stronger variation in specularity coefficient. Consistent with our earlier findings in bubbling fluidized bed, a constant specularity coefficient gives similar results to those using variable specularity coefficients.

Further discussion

The above analysis found that consistent results can be obtained with constant and variable specularity coefficients for both bubbling and circulating fluidized beds. This suggests that an overall effective specularity coefficient might be sufficient for modeling the tangential interaction between the solids flow and the wall. However, as suggested by the results of the variable specularity coefficient model, the distribution of specularity coefficient along the wall is affected by operating conditions, such as superficial gas velocity and solids circulation rate. In addition, the specularity coefficient is also indirectly influenced by other factors affecting the flow hydrodynamics such as drag correlation. Hence, partial-slip boundary conditions with a variable specularity coefficient should be used for accurate numerical simulation, especially for predicting transition between different fluidization regimes. It should be noted that the variable specularity coefficient is developed for interaction between a rapid granular flow and a flat, frictional wall. Hence, it can only account for the small-scale roughness indirectly through the frictional coefficient. However, the resultant strong particle rotations close to the wall are not considered in Eq. 5 as no such information is available in most EE simulations. Without implementing the variable specularity coefficient model into CFD simulations, it is still possible to roughly estimate the range of overall effective specularity coefficient based on the material properties (i.e., friction coefficient and particle-wall restitution coefficient) by using Eq. 6 to calculate the maximum value. Compared to the particle-wall friction coefficient, superficial gas velocity and solids circulation rate showed a relatively weak influence on the overall specularity coefficient, and this also facilitated estimating the overall specularity coefficient beforehand.

When using the variable specularity coefficient, calculation must be done for each wall cell to update the value of specularity coefficient. To evaluate the extra computational cost by the variable specularity coefficient model, computing times for different cases with constant and variable specularity coefficients are compared in Table 5. It is surprising that,

for all cases, the computing time for variable specularity coefficient is slightly shorter than for constant specularity coefficient. It is thought that calculating a variable specularity coefficient along the wall speeds up the convergence of the solution, reducing the computing time slightly. Therefore, we can safely claim that the suggested method of variable specularity coefficient provides additional accuracy without impacting the speed of the calculations.

The 2-D numerical tests here are conducted to study qualitatively the spatial and temporal variation of the specularity coefficient. Although differences exist between 2-D and 3-D numerical simulations of gas–solids fluidized bed,^{19,20} the findings of this current study will probably not be altered by the dimensionality of the problem. Nevertheless, future studies are planned with realistic 3-D numerical simulations to confirm the current findings and validate the model against high-quality experimental data.

Conclusions

The current study demonstrates the importance of solids-phase wall boundary conditions on predicted flow hydrodynamics. Specifically, the effect of specularity coefficient used in Johnson and Jackson partial-slip boundary conditions was discussed. The recently developed model for variable specularity coefficient was implemented and is available in the open-source CFD code, MFIX. Through a series of 2-D numerical simulations of bubbling fluidized bed and circulating fluidized bed riser, the model was qualitatively evaluated and shown to predict consistent trends with previous studies in the literature. The current study examined the spatial and temporal variation of specularity coefficient. It showed that the interaction between solids and wall is affected by the operating conditions such as superficial gas velocity and solids circulation rate.

Furthermore, quantitative comparison between numerical results of variable and constant specularity coefficients was carried out to investigate the effect of spatial and temporal variation in specularity coefficient. It was demonstrated that both constant and variable specularity coefficient predict similar quantitative flow hydrodynamics, provided that the constant value of specularity coefficient is properly set. Overall, the variable specularity coefficient model provides a physically meaningful and direct way to estimate the specularity coefficient that the partial-slip boundary conditions require for the solid phase without increasing the cost of the computation. For CFD codes that do not provide an easy way to implement a variable specularity coefficient, this model also offers a guideline for choosing a rough value for a constant specularity coefficient based on measurable particle–wall collision properties.

Acknowledgments

This technical effort was performed in support of the National Energy Technology Laboratory's ongoing research in advanced multiphase flow simulation under the RES

contract DE-FE0004000. This report was prepared as an account of work sponsored by an agency of the United States Government. Neither the United States Government nor any agency thereof, nor any of their employees, makes any warranty, express or implied, or assumes any legal liability or responsibility for the accuracy, completeness, or usefulness of any information, apparatus, product, or process disclosed, or represents that its use would not infringe privately owned rights. Reference herein to any specific commercial product, process, or service by trade name, trademark, manufacturer, or otherwise does not necessarily constitute or imply its endorsement, recommendation, or favoring by the United States Government or any agency thereof. The views and opinions of authors expressed herein do not necessarily state or reflect those of the United States Government or any agency thereof.

Literature Cited

1. van der Hoef MA, van Sint Annaland M, Deen NG, Kuipers JAM. Numerical simulation of dense gas-solid fluidized beds: a multiscale modeling strategy. *Annu. Rev. Fluid Mech* 2008;40:47–70.
2. Johnson PC, Jackson R. Frictional collisional constitutive relations for antigranulocytes-materials, with application to plane shearing. *J Fluid Mech.* 1987;176:67–93.
3. Jenkins JT. Boundary conditions for rapid granular flows: flat, frictional walls. *J Appl Mech.* 1992;59:120–127.
4. Schneiderbauer S, Schellander D, Loderer A, Pirker S. Non-steady state boundary conditions for collisional granular flows at flat frictional moving walls. *Int J Multiphase Flow.* 2012;43:149–156.
5. Benyahia S, Syamlal M, O'Brien TJ. Evaluation of boundary conditions used to model dilute, turbulent gas/solids flows in a pipe. *Powder Technol.* 2005;156(2–3):62–72.
6. Jin B, Wang X, Zhong W, Tao H, Ren B, Xiao R. Modeling on High-flux circulating fluidized bed with Geldart group B particles by kinetic theory of granular flow. *Energy Fuels.* 2010;24:3159–3172.
7. Lan X, Xu C, Gao J, Al-Dahhan M. Influence of solid-phase wall boundary condition on CFD simulation of spouted beds. *Chem Eng Sci.* 2012;69(1):419–430.
8. Li T, Grace JR, Bi X. Study of wall boundary condition in numerical simulations of 2D bubbling fluidized beds. *Powder Technol.* 2010;203:447–457.
9. Li T, Zhang Y, Grace JR, Bi X. Numerical investigation of gas mixing in gas-solid fluidized beds. *AIChE J.* 2010;56:2280–2296.
10. Wang X, Jin B, Zhong W, Xiao R. Modeling on the hydrodynamics of a high-flux circulating fluidized bed with Geldart group A particles by kinetic theory of granular flow. *Energy Fuels.* 2010;24:1242–1259.
11. Almuttahir A, Taghipour F. Computational fluid dynamics of high density circulating fluidized bed riser: study of modeling parameters. *Powder Technol.* 2008;185(1):11–23.
12. Hui K, Haff PK, Ungar JE. Boundary conditions for high-shear grain flows. *J Fluid Mech.* 1984;145:223–233.
13. Li T, Benyahia S. Revisiting Johnson and Jackson boundary conditions for granular flows. *AIChE J.* 2012;58:2058–2068.
14. Benyahia S, Syamlal M, O'Brien TJ. Summary of MFIx equations 2012-1, 2012; Available at: <https://mfix.netl.doe.gov/documentation/MFIxEquations2012-1.pdf>.
15. Syamlal M, Rogers W, O'Brien TJ. MFIx documentation: theory guide. Morgantown: U.S. Department of Energy (DOE), Morgantown Energy Technology Center, 1993.
16. Syamlal M. MFIx Documentation: Numerical Techniques, Morgantown: U.S. Department of Energy (DOE), Morgantown Energy Technology Center, 1998.
17. Louge MY. Computer simulations of rapid granular flows of spheres interacting with a flat, frictional boundary. *Phys Fluids.* 1994;6:2253.
18. Lu BN, Wang W, Li JH. Eulerian simulation of gas–solid flows with particles of Geldart groups A, B and D using EMMS-based meso-scale model. *Chem Eng Sci.* 2011;66(20):4624–4635.
19. Li T, Gel A, Pannala S, Shahnam M, Syamlal M. CFD simulations of circulating fluidized bed risers, part I: grid study. *Powder Technol.* submitted.
20. Li T, Pannala S, Shahnam M. CFD simulations of circulating fluidized bed risers, part II, evaluation of differences between 2D and 3D simulations. *Powder Technol.* submitted.

Manuscript received Dec. 20, 2012, and revision received Mar. 6, 2013.